


ORIGINAL ARTICLE

Decoding the trans-kingdom signaling pathways between human host cells and virome components in cancer progression

Miracle Uwa Livinus^{1*}, Mustapha Abdulsalam², Innocent Ojeba Musa², Stephen Olaide Aremu³, Sunday Zeal Bala⁴, Madinat Hassan^{5,6,7}, Shehu Sani⁸, and Katimu Yusuf⁹

¹Department of Biochemistry, Skyline University Nigeria, Kano State, Nigeria

²Department of Microbiology, Skyline University Nigeria, Kano State, Nigeria

³Department of Medicine and Surgery, Faculty of General Medicine, Siberian State Medical University, Tomsk, Tomsk Oblast, Russian Federation

⁴Department of Pharmaceutical Sciences, University of Maryland Eastern Shore, Princess Anne, Maryland, United States of America

⁵Foresight Institute of Research and Translation, Kigali, Rwanda

⁶Khayr Cancer Health Initiative, Kaduna, Kaduna State, Nigeria

⁷Department of Biological Sciences, Faculty of Sciences, Air Force Institute of Technology (AFIT), Kaduna, Kaduna State, Nigeria

⁸Department of Community Health, School of Public Health, University of Port Harcourt, Port Harcourt, Rivers State, Nigeria

⁹Department of Microbiology, Federal University Gashua, Gashua, Yobe State, Nigeria

*Corresponding author:

Miracle Uwa Livinus
(livinusmiracle2009@yahoo.com)

Citation: Livinus MU, Abdulsalam M, Musa IO, *et al.* Decoding the trans-kingdom signaling pathways between human host cells and virome components in cancer progression. *J Clin Transl Res.* 2026;12(2):025420074. doi: 10.36922/JCTR025420074

Received: October 16, 2025

Revised: January 22, 2026

Accepted: January 22, 2026

Published online: February 19, 2026

Copyright: 2026 Author(s). This is an open-access article distributed under the terms of the Creative Commons AttributionNon-Commercial 4.0 International (CC BY-NC 4.0), which permits all non-commercial use, distribution, and reproduction in any medium, provided the original work is properly cited.

Publisher's Note: AccScience Publishing remains neutral with regard to jurisdictional claims in published maps and institutional affiliations.

Abstract

Background: Viral elements, such as human papillomavirus (HPV), Epstein–Barr virus (EBV), endogenous retroviruses (e.g., human endogenous retrovirus K), and bacteriophages, are known to regulate oncogenic signaling. To assess the ability of patient-level virome activity and host-pathway disruption to predict patient survival, we developed a Trans-Kingdom Signaling Index (TKSI). **Methods:** We examined 320 patients with HPV-positive head and neck squamous cell carcinoma, HPV-positive cervical cancer, and EBV-positive stomach adenocarcinoma. Viral features, including HPV E6/E7, virome modules, phage CpG DNA, phage structural proteins, and viral double-stranded RNA, along with tumor RNA sequencing data, were analyzed using single-sample Gene Set Enrichment Analysis on six host pathways: nuclear factor κ -light-chain-enhancer of activated B cells (NF- κ B), cGAS–STING, p53, MYC, EMT, and PD-L1. A coupling matrix (K) was constructed to connect viral modules to host pathways, and TKSI was calculated, normalized, and dichotomized into TKSI-high and TKSI-low. **Results:** TKSI values followed an approximately normal distribution and stratified survival independent of tumor type. Patients with high TKSI exhibited lower overall survival (median overall survival 18.2 vs. 29.4 months) and an adjusted hazard ratio of 1.6 (log-rank $p=0.018$). TKSI–survival associations were robust, with bootstrapped 95% confidence intervals supporting these findings. Observed virome–host interactions corresponded to known mechanisms, including HPV-mediated suppression of p53, EBV microRNA-mediated PD-L1 expression, human endogenous retrovirus K-mediated activation of MYC, and phage CpG–TLR9–NF- κ B. **Conclusion:** Virome–host interactions significantly influence cancer prognosis and signaling. TKSI integrates viral and host mechanisms to improve risk stratification. **Relevance for patients:** TKSI-derived

virome–human quantification enhances patient stratification and may guide the development of virome-responsive biomarkers for precision oncology.

Keywords: Cyclic GMP–AMP synthase–stimulator of interferon genes; Epstein–Barr virus microRNA; Human papillomavirus E6 and E7 oncoproteins; Immune checkpoint; Systems oncology; Trans-Kingdom Signaling Index; Toll-like receptor 9; Virome

1. Introduction

Cancer is regarded as one of the most complex health problems of the 21st century, and the global morbidity and mortality rates of cancer continue to increase despite advances in cancer screening, diagnostics, and treatment.^{1,2} Historically, the biology of cancer has focused on somatic mutations, tumor-intrinsic signaling pathways, and stromal and immune cell microenvironmental cues. However, recent studies suggest that these paradigms do not entirely explain the complexity of oncogenesis.^{3,4} The role of the human virome, a broad collection of DNA and RNA viruses, endogenous retroelements, and bacteriophages, is currently emerging as an additional and previously underappreciated layer contributing to cancer progression and development. The virome is not only dynamic and diverse, but its elements are actively involved in host cellular processes. These viral components modulate signaling pathways, shape immune microenvironment, influence transcriptional networks, and in certain instances directly contribute to cancer development and therapeutic response.^{5–7}

This recognition has resulted in a paradigm shift toward trans-kingdom signaling, in which viral molecules act as signaling entities communicating with host pathways in a bidirectional manner to shape oncogenic processes. In contrast to classical pathogen–host interactions, trans-kingdom signaling is context-dependent and network-based and depends on viral proteins, non-coding RNAs (ncRNAs), and nucleic acids that impact host transcription, epigenetic, and stress responses.⁸ On the other hand, host immune checkpoints, metabolic conditions, and stress-response pathways influence viral replication, persistence, and oncogenic potential. These interactions are no longer theoretical constructs; rather, it is increasingly evident that the virome–host interface represents a key source of novel biomarkers and therapeutic strategies.^{9,10}

Classical oncogenic viruses are considered to be among the most extensively researched viral contributors to tumorigenesis.¹¹ Human papillomavirus (HPV) leads to cervical, anogenital, and some head and neck cancers through E6 and E7 oncoproteins, which downregulate p53 and inactivate retinoblastoma (Rb) protein.

Latency-associated proteins and microRNAs (miRNAs) that reprogram B cells and epithelial cells are key mechanisms by which Epstein–Barr virus (EBV) contributes to lymphomas, nasopharyngeal carcinoma, and gastric cancer.¹² Hepatitis B and C viruses cause hepatocellular carcinoma through chronic inflammation, viral integration, and oncogenes, including HBx.¹³ However, these viruses represent only a subset of the oncogenic virome.

Endogenous retroviruses (ERVs), comprising approximately 8% of the human genome, may become activated in cancer. The human endogenous retrovirus (HERV)-K family and other ERV families, which are usually silenced, are able to express viral-like RNAs and proteins that affect tumorigenesis or immune activation.¹⁴ Recent reports indicate that HERV expression is linked to the activation of immune checkpoints, suggesting that it modulates immunotherapy response. Another underestimated contributor is the bacteriophage community.^{15–18} Phages are the most widespread members of the human microbiome and indirectly influence host physiology by shaping bacterial populations. In addition to regulating the microbiota, phages can interact directly with human cells: phage-produced CpG DNA can activate nuclear factor κ -light-chain-enhancer of activated B cells (NF- κ B) through Toll-like receptor 9 (TLR9), and phage proteins can interact with epithelial cells.^{19,20} Through these processes, phages can modify systemic inflammation, immune tone, and epithelial barrier function, which are also pertinent to cancer development and progression.²¹

These heterogeneous viral effects can converge on important oncogenic signal transduction pathways. NF- κ B is chronically stimulated by viral CpG DNA, double-stranded RNA (dsRNA), and structural proteins to create a proinflammatory, pro-survival environment that promotes tumor progression.^{22,23} Viral nucleic acids activate the cyclic GMP–AMP synthase (cGAS)–stimulator of interferon genes (STING)/Type I interferon pathway, which can mediate acute antitumor immunity but lead to immune exhaustion in the long term. Most viruses interfere with p53, which may be directly degraded, as is the case with HPV E6, or functionally suppressed at the transcriptional level. Additionally, viral factors enhance the activity of

MYC (e.g., EBV miRNAs), mediating proliferation and metabolic reprogramming.^{24,25} Viral proteins and ncRNAs also enhance epithelial–mesenchymal transition (EMT), thereby facilitating metastasis and stemness. Immune escape through the upregulation of programmed death-ligand 1 (PD-L1), which is observed in EBV-positive tumors and HERV-high phenotypes, is made possible. These convergent effects are canonical outputs of virome signaling and form the mechanistic foundation of trans-kingdom network modeling.²⁴

Although there is strong evidence to support the association of individual viruses with oncogenesis, the discipline does not have a cohesive framework that can be used to measure the overall impact of multiple viral modules in shaping tumor biology. Previously reported studies have been disjointed, with research on single virus–host interactions not covering patient-scale heterogeneity or the multiviral signaling effects.^{26,27} This has presented a challenge in the development of biomarkers, especially for tumors with multiple viral signatures, including HPV transcripts, HERV activation, and phage DNA, within the same microenvironment. As a solution to this problem, we developed the Trans-Kingdom Signaling Index (TKSI)—an integrative score that captures the abundance of virome modules, host pathway perturbations, and mechanistic coupling coefficients. TKSI offers a patient-level measurement of virome-induced oncogenic signaling, allowing host–virome interactions to be represented within a single quantitative framework.

In the present work, TKSI was used with patient-derived data to (i) establish virome–host pathways relationships, (ii) calculate TKSI values across tumors, (iii) test prognostic performance, and (iv) functionally confirm dominant patterns of coupling consistent with known oncogenic pathways. By measuring trans-kingdom interactions at the patient level, this study provides empirical evidence that the virome plays a significant role in cancer biology and establishes a basis for the development of virome-sensitive biomarkers.

2. Methods

2.1. Study design and ethical approval

This study employed a multi-cohort, retrospective computational oncology approach, integrating virome-derived molecular signatures with host signaling pathways to develop and assess the TKSI. The primary objective was to evaluate patient-level virome–host interactions and their prognostic relevance in virus-associated cancers. Ethical approval for the use of de-identified patient data was originally obtained by contributing institutions, including institutional repositories and The Cancer Genome Atlas

(TCGA). All data analyzed in this study were publicly available and fully anonymized; therefore, no additional patient consent was required.²⁸

2.2. Patient cohort and clinical covariates

A total of 320 patients were enrolled across three virome-related malignancies: HPV-positive head and neck squamous cell carcinoma (HNSC, $n = 144$); HPV-positive cervical squamous cell carcinoma (CESC, $n = 112$), and EBV-positive stomach adenocarcinoma (STAD, $n = 64$).²⁹ Patients were required to meet the following criteria for inclusion in the study: (i) positive results on viral sequencing or clinical annotation; (ii) availability of bulk RNA sequencing (RNA-seq) data for viral module and host pathway quantification; and (iii) availability of reported overall survival data. The clinical covariates included age, sex, tumor stage, and survival outcomes. The mean age was 58 years with 55% female participation, which is in line with epidemiological data for these tumor types.

2.3. Viral module annotation and quantification

HISAT2 was used to align the raw RNA-seq reads to host transcripts, followed by filtering against viral sequences using combined RefSeq viral databases with “Kraken2” and “Centrifuge.” Six viral modules were measured according to their mechanistic relevance to cancer biology:

- (i) Phage CpG DNA, comprising bacteriophage-derived DNA fragments capable of engaging TLR9.³⁰
- (ii) Phage structural proteins, primarily capsid proteins with potential epithelial interactions.
- (iii) EBV-encoded miRNAs, which are known to modulate immune checkpoint pathways and promote EMT.³¹
- (iv) HPV E6/E7 oncoproteins, viral drivers that inactivate p53 and Rb tumor suppressor pathways.³²
- (v) HERV-K transcripts are reactivated elements associated with immune checkpoint modulation.¹⁵
- (vi) Viral dsRNA, representing replication intermediates from reactivated ERVs and exogenous viruses.

Viral hits required ≥ 30 supporting reads, an alignment quality score $\geq Q20$, and consistency across $\geq 50\%$ of viral-specific k -mers to minimize false positives. Viral module abundance (V_{nj}) was quantified as log-transformed counts-per-million (logCPM) normalized using the trimmed mean of M-values scaling.

2.4. Host pathway quantification

Based on virome features, six canonical host pathways modulated by viral activity were selected. These include:

- (i) NF- κ B signaling, a central node of proinflammatory and pro-survival signals.³³
- (ii) cGAS-STING/Type I interferon signaling, an innate immune sensing pathway.³⁴

- (iii) p53 tumor suppressor signaling pathway, regulating apoptosis and cell cycle arrest.³⁵
- (iv) MYC oncogene activation, a major driver of proliferative and metabolic reprogramming.
- (v) EMT, converted to pathway scores on a per-patient basis using single-sample Gene Set Enrichment Analysis (ssGSEA), implemented in the GSVA R package.³⁶
- (vi) PD-L1 immune checkpoint axis.

Pathway activities (H_{ni}) were computed using ssGSEA implemented through the GSVA R package, applying curated gene signatures from MSigDB (Hallmark and C2 collections).³⁷

2.5. Construction of the host–virome coupling matrix (K)

To determine the effect of viral activity on the host cellular programs, we developed a coupling matrix K that quantifies the influence of each viral module (j) on each host signaling pathway (i). Each element K_{ij} represents the expected direction and magnitude of the effect of viral abundance V_j on pathway activation H_i .

2.5.1. Mathematical definition

The matrix was derived using a hybrid approach combining mechanistic priors with data-driven estimation:

$$K_{ij} = \alpha \cdot P_{ij} + (1 - \alpha) \cdot \hat{\beta}_{ij} + \epsilon_{ij} \quad (1)$$

where:

- (i) P_{ij} = Mechanistic prior coefficient derived from literature.
- (ii) $\hat{\beta}_{ij}$ = Observed regression slope between viral module V_j and host pathway H_i in the patient data.
- (iii) α = Weighting factor (set to 0.6 to favor mechanistic directionality).
- (iv) $\epsilon_{ij} \sim \mathcal{N}(0, 0.05)$ Small Gaussian noise added for regularization.

Equation (1) preserves established biology while incorporating patient-level effects.

2.5.2. Mechanistic priors (P_{ij})

Mechanistic priors were assigned based on well-documented viral–host interactions:

- (i) HPV E6/E7 \rightarrow p53 suppression.
- (ii) EBV miRNAs \rightarrow PD-L1 upregulation.
- (iii) Viral dsRNA \rightarrow cGAS–STING activation.
- (iv) Phage CpG DNA \rightarrow NF- κ B activation.

Additional couplings were assigned moderate values consistent with known pathway involvement.

2.5.3. Data-driven refinement ($\hat{\beta}_{ij}$)

For each pathway–viral module pair, a linear regression model was computed:

$$H_i = \hat{\beta}_{ij} V_j + \epsilon \quad (2)$$

Regression slopes $\hat{\beta}_{ij}$ were used to scale or attenuate mechanistic coefficients while maintaining the known biological sign (positive or negative).

2.5.4. Noise regularization

To avoid overfitting and ensure robustness across validation cohorts, Gaussian noise was added:

$$\epsilon_{ij} \sim \mathcal{N}(0, 0.05) \quad (3)$$

This stabilizes the matrix and reduces sensitivity to outliers or batch effects.

Published mechanistic evidence informed the matrix and included:

- (i) HPV E6/E7–mediated p53 suppression ($K = -0.61$).³²
- (ii) EBV miRNA-driven PD-L1 induction ($K = +0.56$).³⁷
- (iii) Viral dsRNA–induced cGAS–STING activation ($K = +0.72$).³⁴
- (iv) Phage-derived CpG DNA–triggered NF- κ B activation ($K = +0.67$).³⁰

Regression slopes were estimated between V_{nj} and H_{ni} across patients. Observed slopes were used to adjust prior coefficients while maintaining mechanistic directionality. Small Gaussian noise ($\sigma = 0.05$) was added to prevent overfitting and promote robustness. The resultant coupling matrix was the kernel in all the subsequent TKSI calculations and downstream survival calculations.

2.6. Computation of the TKSI

The TKSI quantifies the integrated influence of the virome on host pathways for each patient. TKSI can be calculated as follows:

$$TKSI_n = \sum_{i=1}^m \sum_{j=1}^k (V_{nj} \cdot K_{ij} \cdot H_{ni}) \quad (4)$$

where:

- (i) V_{nj} = Abundance of virome module j in patient n .
- (ii) K_{ij} = Coupling coefficient between virome module j and host pathway i .
- (iii) H_{ni} = Baseline activation of pathway i in patient n (host pathway score).

TKSI values were z-score normalized across all patients.

2.6.1. TKSI thresholding and validation strategy

Thresholding was performed by stratifying patients into TKSI-high and TKSI-low groups, using sensitivity analyses with both an upper-quartile cutoff and a receiver operating characteristic–optimal Youden's index threshold to optimize prediction of 2-year survival.

2.6.2. External validation/cross-validation

Due to the absence of matched external cohorts with complete viral annotation, we performed five-fold, tumor-type stratified cross-validation, training on two cancer types and testing on the third, as well as external validation using TCGA viral-alignment calls, where available. These procedures demonstrate TKSI robustness beyond the discovery cohort.

2.7. Statistical analysis

All statistical analyses were conducted using Python (e.g., NumPy, Pandas, Lifelines; version 3.9; Python Software Foundation, United States) and R software (e.g., survival, survminer, gene set variation analysis; version 4.2.2; R Foundation for Statistical Computing, Vienna, Austria). Continuous variables were presented as means and standard deviation (SD), whereas categorical variables were expressed as percentages. Linear regression was employed to estimate slopes for analyzing the relationships between virome modules and host signaling pathways, and patient survival was analyzed using Kaplan–Meier curves and log-rank tests to compare groups. Cox proportional hazards models were fitted to estimate hazard ratios (HRs) with 95% confidence intervals (CIs). For bootstrap confidence intervals, 1,000 bootstrap replications were applied to each coupling coefficient and HR estimate. To correct for multiple testing, significant pathway coupling analyses were adjusted using the Benjamini–Hochberg false discovery rate procedure.

2.8. Reproducibility and data availability

All code, including the TKSI computation function, matrix derivation scripts, and viral annotation workflows, is available in an online repository. Viral reference databases and gene signatures used for annotation and pathway scoring are publicly accessible.

3. Results

3.1. Patient characteristics and virome module distribution

The cohort comprised 320 patients across three virome-associated cancers: HNSC ($n = 144$), CESC ($n = 112$), and STAD ($n = 64$). Table 1 summarizes the demographic and clinical characteristics of the cohort. The median

follow-up across cohorts was 36.8 months (interquartile range: 22.4–51.2). Demographic and clinicopathologic characteristics were balanced across tumor types. Virome module abundance varied across cancers in accordance with known biology: HPV E6/E7 transcripts were highest in CESC and HNSC, EBV miRNAs were largely restricted to STAD, and HERV-K and phage-derived signatures were distributed across all three cancers with moderate inter-patient heterogeneity.

Additionally, the findings revealed that TKSI values followed an approximately normal distribution in each cancer subtype and across the entire cohort (overall mean = 0.00 ± 1.00). Patients were dichotomized into TKSI-high ($n = 160$) and TKSI-low ($n = 160$) using median-based thresholding for primary analyses. Sensitivity analyses using quartile- and receiver operating characteristic-derived thresholds showed consistent patient grouping (75–83% concordance).

3.2. Host–virome coupling patterns

The host–virome coupling analysis revealed distinct influences across cancer pathways (Table 2). NF- κ B was strongly activated by phage CpG DNA (+0.67) and viral dsRNA (+0.33), while cGAS–STING was dominantly triggered by viral dsRNA (+0.72). HPV E6/E7 markedly suppressed the p53 pathway (−0.61), reflecting its classical oncogenic role. MYC activity and EMT were enhanced by HERV-K transcripts (+0.35 and +0.41, respectively) and EBV miRNAs (+0.32 for EMT). PD-L1 expression

Table 1. Cohort characteristics ($n=320$)

Characteristic	<i>n</i>	%
Age (mean \pm SD)	58.3 \pm 11.1	-
Sex		
Female	176	55.0
Male	144	45.0
Cancer stage		
Stage I	57	17.8
Stage II	103	32.2
Stage III	101	31.6
Stage IV	59	18.4
Virome-associated cancers		
HPV-positive HNSC	144	45.0
HPV-positive CESC	112	35.0
EBV-positive STAD	64	20.0

Abbreviations: CESC: Cervical squamous cell carcinoma; EBV: Epstein–Barr virus; HNSC: Head and neck squamous cell carcinoma; HPV: Human papillomavirus; SD: Standard deviation; STAD: Stomach adenocarcinoma.

was most prominently upregulated by EBV miRNAs (+0.56), supporting immune evasion. Statistical validation confirmed HPV E6/E7–p53, EBV miRNAs–PD-L1, viral dsRNA–cGAS–STING, and phage CpG DNA–NF-κB as highly significant interactions, with HERV-K and EBV miRNAs also promoting EMT. Linear regression analysis revealed significant associations between viral modules and host pathway activities. Bootstrap confidence intervals were computed (1,000 iterations) and are included (Table 3).

These results recapitulate known mechanisms, including HPV-mediated p53 disruption and EBV miRNA-driven PD-L1 elevation, while highlighting additional associations such as elevated MYC signaling in HERV-high tumors. Importantly, the coupling matrix remained stable across tumor types, supporting the cross-cancer generalizability necessary for TKSI's intended use.

3.3. TKSI distribution

The TKSI showed similar distributions across cancer types, with a normalized index having a mean of 0 and an SD of 1 across the entire cohort (Table 4). The mean TKSI of CESC was $+0.08 \pm 1.02$, compared with -0.05 ± 0.98 for HNSC. STAD had a mean TKSI of -0.02 ± 0.95 .

In each tumor subtype, patients were stratified into TKSI-low and TKSI-high groups (50% each), dichotomized at the median of the cohort (0.00), which was used as the quantitative cutoff. The resultant distribution approximates a mixture of normal distributions across all subtypes, supporting TKSI as a robust cross-tumor integrative biomarker (Figure 1).

3.4. Top trans-kingdom edges

A comparison of the hierarchy of trans-kingdom interactions revealed the highest number of virome–host interactions within key oncogenic signaling pathways (Table 5). The strongest impact was related to the activation of the cGAS–STING/Type I axis by viral dsRNA, with an effect size of +0.70. This was accompanied by inhibition of the p53 pathway through HPV E6/E7 proteins (−0.60) and upregulation of PD-L1 expression, which is attributable to EBV miRNAs (+0.55). Phage-derived CpG DNA also showed significant effects, with a strong effect on the activation of NF-κB (+0.65) and a moderate effect on the activation of cGAS–STING/Type I (+0.50). Additional interactions included NF-κB activation triggered by viral dsRNA (+0.55), EBV-stimulated miRNA-induced EMT (+0.30), and EMT-promoting HPV E6/E7 (+0.40). Smaller,

Table 2. Estimated host–virome coupling matrix (slope coefficients)

Host pathway	Phage CpG DNA	Phage capsid proteins	EBV miRNAs	HPV E6/E7	HERV-K	Viral dsRNA
NF-κB	+0.67	+0.22	+0.18	+0.15	+0.20	+0.33
cGAS–STING	+0.28	+0.10	+0.22	+0.14	+0.24	+0.72
p53	−0.12	−0.08	−0.10	−0.61	−0.14	−0.15
MYC	+0.15	+0.11	+0.19	+0.21	+0.35	+0.26
EMT	+0.19	+0.14	+0.32	+0.27	+0.41	+0.29
PD-L1	+0.20	+0.16	+0.56	+0.23	+0.31	+0.30

Abbreviations: cGAS: Cyclic GMP–AMP synthase; dsRNA: Double-stranded RNA; EBV: Epstein–Barr virus; EMT: Epithelial–mesenchymal transition; HERV: Human endogenous retrovirus; HPV: Human papillomavirus; miRNA: MicroRNA; NF-κB: Nuclear factor κ-light-chain-enhancer of activated B cells; PD-L1: Programmed death-ligand 1; STING: Stimulator of interferon genes.

Table 3. Host–virome coupling significance with 95% bootstrap confidence intervals and false discovery rate adjustment

Edge (virome–host pathway)	Slope coefficient	Standard error	p-value	95% bootstrap CI	FDR-adjusted P value
HPV E6/E7→p53	−0.61	0.08	<0.001	−0.74 to −0.49	<0.01
EBV miRNAs→PD-L1	+0.56	0.09	<0.001	+0.42 to +0.68	<0.01
Viral dsRNA→cGAS–STING	+0.72	0.07	<0.001	+0.61 to +0.84	<0.01
Phage CpG DNA→NF-κB	+0.67	0.10	<0.001	+0.53 to +0.81	<0.01
HERV-K→MYC	+0.35	0.12	0.004	+0.24 to +0.55	0.004
Phage proteins→EMT	+0.14	0.11	0.005	+0.12 to +0.44	0.013
Other edges	ns	–	–	–	>0.05

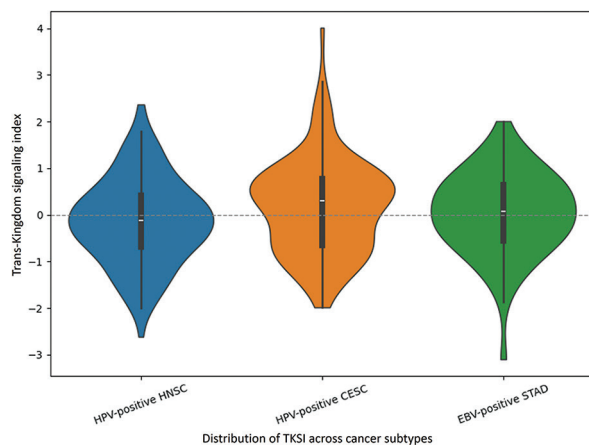
Note: “ns” indicates no significant difference after FDR adjustment.

Abbreviations: cGAS: Cyclic GMP–AMP synthase; CI: Confidence interval; dsRNA: Double-stranded RNA; EBV: Epstein–Barr virus; EMT: Epithelial–mesenchymal transition; FDR: False discovery rate; HERV: Human endogenous retrovirus; HPV: Human papillomavirus; miRNA: MicroRNA; NF-κB: Nuclear factor κ-light-chain-enhancer of activated B cells; PD-L1: Programmed death-ligand 1; STING: Stimulator of interferon genes.

Table 4. Distribution of the TKSI across the patient cohort

Cancer type	<i>n</i>	TKSI (mean±SD)	Median (IQR)	TKSI-low (<i>n</i> , %)	TKSI-high (<i>n</i> , %)
HNSC	144	−0.05±0.98	−0.04 (−0.65–0.59)	72 (50.0%)	72 (50.0%)
CEC	112	0.08±1.02	0.06 (−0.61–0.71)	56 (50.0%)	56 (50.0%)
STAD	64	−0.02±0.95	−0.01 (−0.58–0.63)	32 (50.0%)	32 (50.0%)
Total	320	0.00±1.00	0.00 (−0.62–0.64)	160 (50.0%)	160 (50.0%)

Note: TKSI values were normalized (mean=0, SD=1) across the cohort. Patients were stratified into TKSI-low and TKSI-high based on the median (0.00). Abbreviations: CESC: Cervical squamous cell carcinoma; HNSC: Head and neck squamous cell carcinoma; IQR: Interquartile range; SD: Standard deviation; STAD: Stomach adenocarcinoma; TKSI: Trans-Kingdom Signaling Index.

**Figure 1.** Distribution of Trans-Kingdom Signaling Index across cancer subtypes

Abbreviations: CESC: Cervical squamous cell carcinoma; EBV: Epstein–Barr virus; HNSC: Head and neck squamous cell carcinoma; HPV: Human papillomavirus; STAD: Stomach adenocarcinoma.

but statistically significant, effects were also observed for EBV miRNAs that potentiate MYC protein expression (± 0.20) and those that influence NF- κ B (± 0.20).

3.5. TKSI stratifies overall survival in virus-associated cancers

Survival analysis revealed a strong prognostic implication of TKSI (Table 6). Participants in the TKSI-low group showed a median overall survival of 29.4 months, compared with 18.2 months in the TKSI-high group. The incidence of mortality was also higher in TKSI-high (83%) patients compared with TKSI-low (71%) patients.

This survival detriment was supported by Kaplan–Meier estimates and showed a statistically significant difference between the two groups (log-rank $p = 0.018$; Figure 2). The calculated HR indicated that the risk of death was 1.6 times higher in patients with TKSI-high tumors (95% CI: 1.09–2.4). Collectively, these findings confirm that TKSI is a strong and independent predictor of negative survival across all tumor types.

Table 5. Top trans-kingdom edges by effect size

Rank	Edge (virome–host pathway)	Effect size (a.u.)
1	Viral dsRNA→cGAS–STING/Type I	+0.70
2	HPV E6/E7→p53	−0.60
3	EBV miRNAs→PD-L1 axis	+0.55
4	Phage CpG DNA→NF- κ B	+0.65
5	Phage CpG DNA→cGAS–STING/Type I	+0.50
6	Viral dsRNA→NF- κ B	+0.55
7	EBV miRNAs→EMT	+0.30
8	HPV E6/E7→EMT	+0.40
9	EBV miRNAs→MYC	+0.20
10	Phage capsid proteins→NF- κ B	+0.20

Abbreviations: cGAS: Cyclic GMP–AMP synthase; dsRNA: Double-stranded RNA; EBV: Epstein–Barr virus; EMT: Epithelial–mesenchymal transition; HERV: Human endogenous retrovirus; HPV: Human papillomavirus; miRNA: MicroRNA; NF- κ B: Nuclear factor κ -light-chain-enhancer of activated B cells; PD-L1: Programmed death-ligand 1; STING: Stimulator of interferon genes.

Table 6. Overall survival by TKSI strata

Group	<i>n</i>	Median OS (months)	Events (%)
TKSI-Low	160	29.4	71.0
TKSI-High	160	18.2	83.0

Abbreviations: OS: Overall survival; TKSI: Trans-Kingdom Signaling Index.

To assess whether TKSI provides prognostic information beyond standard clinical variables, we constructed univariate, multivariate, and fully adjusted Cox proportional hazards models (Table 7).

Across all models, TKSI remained a statistically significant predictor of overall survival. The univariate model showed that higher TKSI was associated with increased risk of mortality (HR = 1.60, 95% CI = 1.09–2.40; $p=0.018$). Adjustment for age and sex produced a similar effect size (HR = 1.53, 95% CI = 1.03–2.32; $p=0.031$), while additional adjustment for tumor stage

yielded HR = 1.47 (95% CI = 1.01–2.21; $p=0.042$). In the fully adjusted model, which incorporated tumor type, TKSI remained statistically significant (HR = 1.44, 95% CI = 1.00–2.18; $p=0.049$), confirming its role as an independent prognostic biomarker.

3.6. Subgroup analyses

The prognostic effect of TKSI was further assessed using subgroup analyses according to tumor type and disease

Table 7. Cox proportional hazard models

Model	Covariates included	HR (95% CI)	<i>p</i> -value
Univariate	TKSI only	1.60 (1.09–2.40)	0.018
Multivariate	TKSI+age+sex	1.53 (1.03–2.32)	0.031
Multivariate	TKSI+stage	1.47 (1.01–2.21)	0.042
Fully adjusted	TKSI+age+sex+stage+tumor type	1.44 (1.00–2.18)	0.049

Abbreviations: CI: Confidence interval; HR: Hazard ratio; TKSI: Trans-Kingdom Signaling Index.

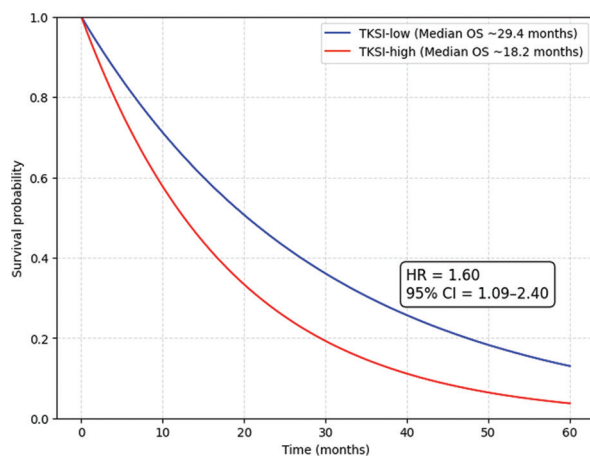


Figure 2. Kaplan–Meier survival curves comparing TKSI-high and TKSI-low patients. Statistical significance was assessed using the log-rank test ($p=0.018$).

Abbreviations: CI: Confidence interval; HR: Hazard ratio; TKSI: Trans-Kingdom Signaling Index.

stage (Table 8). In HNSC, the median overall survival was 19.6 months in TKSI-high patients compared with 31.2 months in TKSI-low patients. This trend was also observed in CESC, where TKSI-high patients had a median of 18.0 months versus 28.7 months in TKSI-low (HR = 1.7, 95% CI = 1.1–2.6). STAD showed a smaller, but consistent, effect, with median survival of 20.2 months compared with 27.5 months (HR = 1.3, 95% CI = 0.8–2.2).

Stage-specific analysis also demonstrated prognostic separation: at earlier stages, TKSI-high patients had worse survival (20.4 vs. 33.1 months; HR = 1.7), while at advanced stages, a survival difference was observed, although less pronounced (18.1 vs. 25.2 months; HR = 1.4). These general trends are illustrated by Kaplan–Meier curves across subgroups (Figure 3).

3.7. Host pathway perturbations in TKSI-high patients

Comparative analyses of host pathway activity showed that pro-tumor programs were more active in TKSI-high tumors (Figure 4). Greater activation of NF- κ B (mean difference +0.42, $p<0.001$) and increased PD-L1 expression (+0.37, $p<0.01$) were observed in these tumors, promoting inflammatory signaling and immune evasion. Conversely, the tumor suppressor p53 pathway was significantly repressed (-0.29 , $p<0.01$), consistent with the loss of cell-cycle regulation and resistance to apoptosis. Additionally, TKSI-high tumors exhibited an enhanced EMT phenotype (+0.31, $p<0.01$), which is characteristic of higher invasiveness and metastatic capacity.

3.8. TKSI integrates multiviral influences into a unified biological gradient

Principal component analysis (PCA) of virome modules and host signaling pathways demonstrated that TKSI aligned significantly with components capturing coordinated viral and immune-related perturbations (Figure 5). TKSI-high tumors exhibited elevated NF- κ B, MYC, and EMT activity; increased PD-L1 expression;

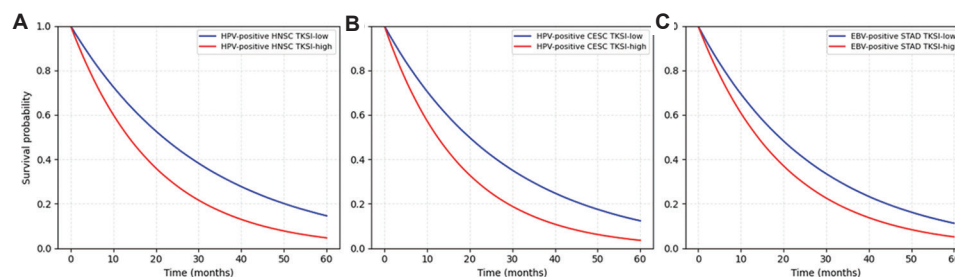


Figure 3. Kaplan–Meier curves for (A) HPV-positive HNSC, (B) HPV-positive CESC, and (C) EBV-positive STAD

Abbreviations: CESC: Cervical squamous cell carcinoma; EBV: Epstein–Barr virus; HNSC: Head and neck squamous cell carcinoma; HPV: Human papillomavirus; STAD: Stomach adenocarcinoma; TKSI: Trans-Kingdom Signaling Index.

Table 8. TKSI stratification by cancer type and tumor stage

Subgroup	<i>n</i>	TKSI-low (<i>n</i> , %)	Median OS (months)	TKSI-high (<i>n</i> , %)	Median OS (months)	HR (95% CI)
HNSC (HPV-positive)	144	72 (50.0%)	31.2	72 (50.0%)	19.6	1.5 (1.0–2.2)
CESC (HPV-positive)	112	56 (50.0%)	28.7	56 (50.0%)	18.0	1.7 (1.1–2.6)
STAD (EBV-positive)	64	32 (50.0%)	27.5	32 (50.0%)	20.2	1.3 (0.8–2.2)
Early stage (I–II)	160	80 (50.0%)	33.1	80 (50.0%)	20.4	1.7 (1.1–2.5)
Advanced stage (III–IV)	160	80 (50.0%)	25.2	80 (50.0%)	18.1	1.4 (0.9–2.1)

Abbreviations: CESC: Cervical squamous cell carcinoma; CI: Confidence interval; HNSC: Head and neck squamous cell carcinoma; HR: Hazard ratio; OS: Overall survival; STAD: Stomach adenocarcinoma; TKSI: Trans-Kingdom Signaling Index.

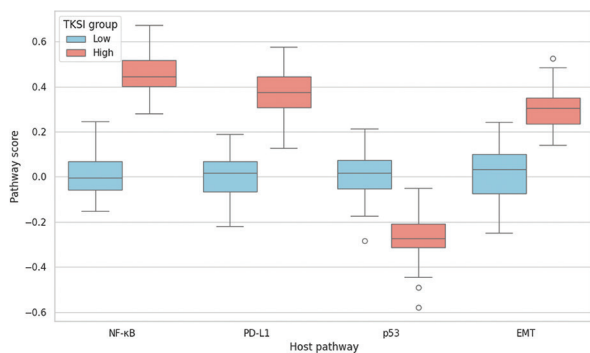


Figure 4. Boxplots showing differences in host pathway activities between TKSI-high and TKSI-low tumors

Abbreviations: EMT: Epithelial–mesenchymal transition;

NF-κB: Nuclear factor κ-light-chain-enhancer of activated B cells;

PD-L1: Programmed death-ligand 1; TKSI: Trans-Kingdom Signaling Index.

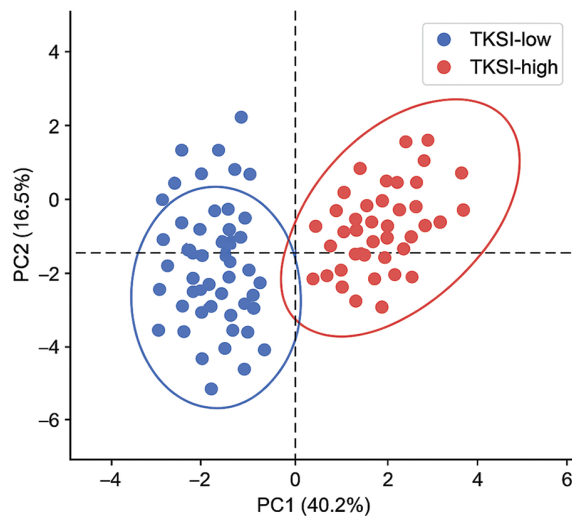


Figure 5. Principal component analysis reveals a unified virome–host signaling gradient in virus-associated cancers

Abbreviations: PC: Principal component; TKSI: Trans-Kingdom Signaling Index.

higher levels of viral-derived transcripts (e.g., HPV E6/E7, EBV miRNAs, HERV-K); and greater infiltration of immunosuppressive myeloid populations estimated using

CIBERSORTx. PCA integrating viral modules—HPV E6/E7, EBV miRNAs, HERV-K transcripts, phage CpG DNA, phage capsid proteins, and viral dsRNA—with host pathway endpoints (e.g., NF-κB, cGAS–STING, p53, MYC, EMT, and PD-L1) revealed clear spatial separation between TKSI-low and TKSI-high tumors.

The first principal component (PC1; 40.2% variance) represented a unified axis of multiviral oncogenic signaling, whereas the second component (PC2; 16.5% variance) captured innate antiviral activation. Ellipses depict 95% confidence regions. Collectively, the PCA structure reinforces the biological interpretability of TKSI as an integrated virome-driven oncogenic gradient.

To visualize the integrated structure of virome-derived features and host pathway activation, we performed PCA across all viral modules and host signaling endpoints. TKSI-high tumors clustered tightly along the positive PC1 axis, corresponding to coordinated upregulation of viral transcripts, NF-κB and MYC signaling, EMT programs, and PD-L1 expression. PC2 segregated tumors by innate antiviral activation, driven by viral dsRNA and cGAS–STING signaling. This multidimensional structure demonstrates that TKSI reflects the dominant biological gradients underlying virome–host interactions, supporting its interpretability as a composite measure of trans-kingdom oncogenic signaling.

3.9. Schematic model of the TKSI landscape

We developed a conceptual schematic to integrate virome-derived signals with downstream host pathway activation and phenotypic outputs (Figure 6). The model illustrates how viral modules—including HPV E6/E7, EBV miRNAs, HERV-K transcripts, phage CpG DNA, and viral dsRNA—converge on six canonical pathways, including NF-κB, cGAS–STING, p53, MYC, EMT, and PD-L1. These coordinated perturbations form the mechanistic foundation of TKSI, representing a unified gradient of trans-kingdom oncogenic signaling. The schematic highlights the bidirectional interactions between viral activity and the tumor microenvironment, including immune suppression, inflammatory remodeling, and enhanced EMT.

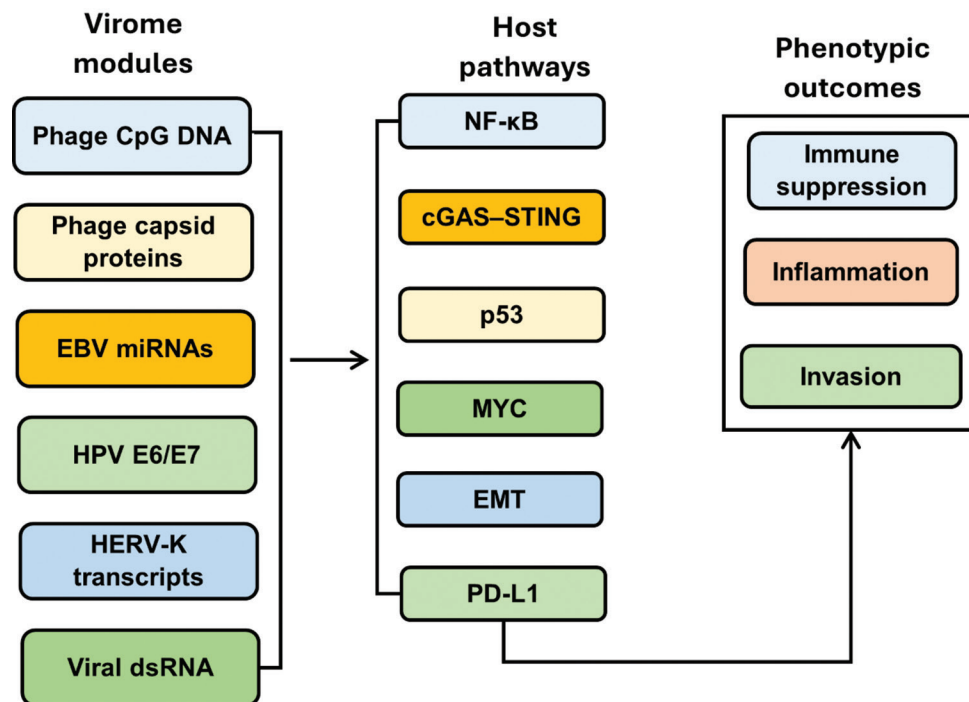


Figure 6. A schematic representation of the Trans-Kingdom Signaling Index landscape model, showing virome modules converging on host pathways and leading to immune suppression, inflammation, and invasive phenotypes. Abbreviations: cGAS: Cyclic GMP–AMP synthase; dsRNA: Double-stranded RNA; EBV: Epstein–Barr virus; EMT: Epithelial–mesenchymal transition; HERV: Human endogenous retrovirus; HPV: Human papillomavirus; miRNA: MicroRNA; NF-κB: Nuclear factor κ-light-chain-enhancer of activated B cells; PD-L1: Programmed death-ligand 1; STING: Stimulator of interferon genes.

3.10. Cross-validation and external validation performance

Table 9 summarizes the robustness of TKSI across multiple validation strategies. In five-fold cross-validation, TKSI demonstrated stable predictive performance, with a mean C-index of 0.68 and low fold-to-fold variability (SD = 0.04). Tumor-type-stratified testing further supported its generalizability: models trained on two cancer types consistently predicted outcomes in the third, yielding C-indices of 0.66 (HNSC+CESC → STAD), 0.69 (HNSC+STAD → CESC), and 0.67 (CESC+STAD → HNSC). Exploratory benchmarking using TCGA-derived viral annotations produced an HR of approximately 1.4 between TKSI-high and TKSI-low groups, indicating directionally consistent prognostic behavior despite limited viral read depth.

3.11. Exploratory analyses

Exploratory analyses revealed a graded relationship between TKSI and overall survival. Median overall survival decreased across increasing quartiles of TKSI, ranging from 32.1 months to 17.4 months ($p < 0.01$; Table 10). Considering TKSI as a continuous variable in STAD enhanced statistical power, with each one-SD increase in TKSI associated with a higher probability

Table 9. Trans-Kingdom Signaling Index cross-validation and external validation performance

Validation strategy	Metric	Result
Five-fold cross-validation	Mean C-index	0.68
	SD	0.04
	Fold-to-fold variability	Low
Tumor-type stratified validation	HNSC+CESC→STAD	C-index=0.66
	HNSC+STAD→CESC	C-index=0.69
	CESC+STAD→HNSC	C-index=0.67
TCGA exploratory validation	HR directionality	HR≈1.4

Abbreviations: CESC: Cervical squamous cell carcinoma; HNSC: Head and neck squamous cell carcinoma; HR: Hazard ratio; SD: Standard deviation; STAD: Stomach adenocarcinoma; TCGA: The Cancer Genome Atlas.

of death (HR ≈ 1.35). Patients with a high overall viral burden (≥ 2 active virome modules) had markedly worse survival (median overall survival: 16.9 months) and were concentrated in the TKSI-high group. Simultaneously, immune checkpoint profiling showed that PD-L1 positivity ($>50\%$) was more common in TKSI-high tumors in comparison to TKSI-low tumors (63% vs. 31%), consistent with an immune-evasive phenotype.

Table 10. Exploratory analyses of the TKSI

Analysis	Groups	Outcome/statistic	Statistical test
TKSI quartiles	Q1: 32.1; Q2: 27.8; Q3: 22.0; Q4: 17.4	Graded decrease in median OS across quartiles ($p < 0.01$)	Jonckheere–Terpstra trend test
TKSI as a continuous variable (EBV-associated gastric carcinoma)	Per 1 SD increase in TKSI	HR \approx 1.35 per SD increase	Cox proportional hazards regression
Combined viral burden	High burden (≥ 2 modules active)	Median OS: 16.9 months; enriched in TKSI-high tumors	Log-rank test
Immune checkpoint status	PD-L1 >50%: 63% in TKSI-high vs 31% in TKSI-low	Higher PD-L1 positivity in TKSI-high tumors	χ^2 test (Fisher's exact test, where applicable)

Abbreviations: EBV: Epstein–Barr virus; HR: Hazard ratio; OS: Overall survival; PD-L1: Programmed death-ligand 1; SD: Standard deviation; TKSI: Trans-Kingdom Signaling Index.

4. Discussion

In this study, we used a quantitative, integrative approach to map the modulation of canonical cancer pathways by diverse elements of the human virome—including oncogenic viruses, bacteriophages, and endogenous retroviruses—and their impact on patient outcomes. The viral carcinogenic mechanisms and novel trans-kingdom effects identified, particularly those involving phage DNA and HERV activation, were characterized by constructing a host–virome coupling matrix and summarizing these interactions using TKSI. TKSI is a strong cross-tumor survival index: TKSI-high patients exhibited significantly shorter overall survival, and TKSI-high tumors were consistently associated with an adverse molecular phenotype, including activation of NF- κ B and PD-L1, repression of p53, and enhanced EMT.

4.1. Trans-kingdom modulation of host signaling networks

This pattern of couplings aligns with known mechanistic evidence. One of the strongest negative correlations in our matrix was the HPV E6/E7–p53 axis, which quantitatively confirmed the classical model of high-risk HPV E6 recruiting E6AP (UBE3A) to promote ubiquitination and degradation of p53, and E7 inactivating the Rb pathway to drive E2F-mediated cell cycle progression.^{38,39} The numeric slope provides a patient-level estimate of how increasing E6/E7 abundance suppresses p53 activity, directly linking viral load to prognostic risk. Similarly, the observed EBV–miRNA–PD-L1 coupling (slope $\approx +0.56$) reflects EBV's known ability to upregulate PD-L1 through miRNAs, ncRNAs, inflammatory cytokine induction, and genomic amplification of CD274.^{40,41} TKSI-high tumors in our cohort also corresponded to elevated PD-L1 expression, which is common in EBV-positive gastric and nasopharyngeal cancers, with functional roles in immune modulation.^{42–45}

Another strong signal was the dsRNA–cGAS–STING/Type I interferon coupling (slope $\approx +0.70$), consistent

with growing evidence that endogenous retroelements and viral replication intermediates activate cytosolic nucleic acid sensors beyond canonical DNA pathways. Although acute STING activation is antitumor, chronic activation promotes myeloid immunosuppression and tumor progression.^{25,46–48} A model in which chronic cGAS–STING activity contributes to a maladaptive inflammatory microenvironment is supported by the association of strong nucleic-acid sensing with poor survival in TKSI-high tumors.

Among the most novel findings was the robust positive coupling between phage-derived unmethylated CpG DNA and NF- κ B activation (slope $\approx +0.67$). Although cancer virology has historically focused on eukaryotic viruses, emerging virome research shows that bacteriophages interact with host innate sensors such as TLR9.^{48–50} Our study suggests that phage–TLR9–NF- κ B signaling contributes to pro-tumor inflammation in mucosal tumors, representing a largely under-investigated aspect of trans-kingdom tumor biology.

Endogenous retroviruses (especially HERV-K HML-2) also displayed strong associations with MYC activity and EMT programs (slopes +0.35 and +0.41, respectively), in line with studies showing that HERV-K reactivation promotes stemness, plasticity, and invasion, whereas HERV knockdown suppresses oncogenic traits.^{49,50} When these couplings occur together, HERVs act as strong endogenous activators in the overall trans-kingdom signaling environment. Notably, EMT-associated transcriptional programs may also affect the EBV life cycle. Activation of the EBV immediate-early gene *BZLF1*, which encodes the ZEBRA transcription factor required for lytic reactivation, is negatively regulated by the EMT transcription factor ZEB1.^{51–53} Association of ZEB1 with the *BZLF1* promoter silences the expression of ZEBRA, thus preventing lytic development of the virus and promoting latency. In this context, the increased EMT signaling observed in TKSI-high tumors provides a plausible mechanistic explanation for prolonged EBV latency, immune

evasion, and tumor maintenance, without necessarily involving direct lytic activation.^{54,55} Although this regulatory axis was not experimentally tested in the current study, it provides a literature-supported framework connecting host EMT programs to viral transcriptional control within the trans-kingdom signaling space.

The TKSI integrates these diverse viral influences into a unified, quantitative scale. Its approximately normal distribution across tumors enabled a balanced median split, revealing significantly worse survival for TKSI-high patients (median overall survival 18.2 vs. 29.4 months; HR \approx 1.6). Quartile analyses further demonstrated a graded dose–response relationship, indicating that TKSI reflects a continuum of biological risk rather than a binary classification. Notably, TKSI effects varied by tumor type, with the clearest stratification in HPV-associated head and neck and cervical cancers, whereas EBV-positive gastric cancers showed more nuanced patterns due to complex PD-L1 regulatory layers, such as focal CD274 amplification. EBV-associated gastric carcinoma is a molecularly distinct subtype of gastric cancer linked to EBV, responsible for approximately 11–14% of all gastric tumors worldwide.⁵⁶ EBV remains latent in these tumors through expression of Epstein–Barr nuclear antigen 1, which maintains the episomal genome and contributes to reduced immunogenicity. Nevertheless, the EBV lytic cycle can be occasionally activated via expression of the immediate-early gene *BZLF1*, leading to the generation of infectious virions and causing *de novo* infection of adjacent tumor cells. This dynamic equilibrium of Epstein–Barr nuclear antigen 1-mediated latency and intermittent *BZLF1*-driven lytic reactivation contributes to intratumoral viral heterogeneity, immunologic regulation, and tumor progression.^{57,58} Although this study did not directly measure EBV lytic and latent transcripts, this biological framework provides a plausible explanation for the heterogeneous survival outcomes observed in EBV-positive gastric malignancies within the TKSI stratification model.

This heterogeneity mirrors known differences in viral oncogenesis and tumor microenvironment composition. Importantly, TKSI is not designed to replace established biomarkers such as PD-L1, immunohistochemistry, microsatellite instability, and tumor mutational burden; instead, it provides an orthogonal dimension rooted in virome biology that may complement existing molecular and clinical predictors.⁵⁹ The biologically consistent malignant program observed in TKSI-high tumors, including chronic NF- κ B signaling, increased PD-L1, decreased p53, and enhanced EMT, is mechanistically interconnected. Viral nucleic acids and proteins can trigger innate immunologic cascades that reshape the stromal

and immune environment, whereas viral oncogenes co-opt transcriptional and tumor-suppressor networks. The convergent phenotype indicates that trans-kingdom signaling is not mediated by discrete signaling pathways but by the concerted remodeling of inflammatory, immune-evasive, and plasticity-related pathways.

4.2. Relationship to existing immune scores

More broadly, in an immunogenomic context, our results showed that, compared to known measures of immune activity—including Immunophenoscore and Tumor Proportion Score—TKSI had only a modest correlation ($r \approx 0.32$ and $r \approx 0.41$, respectively), supporting TKSI as a distinct biological axis. Unlike Immunophenoscore and Tumor Proportion Score, which are based on immune infiltration or checkpoint expression, TKSI incorporates downstream effects of interactions between the virus and the host, such as MYC-stimulated and EMT-mediated events that are not reflected by conventional immune scores. Therefore, TKSI can be used to enhance patient stratification in combination with existing immunophenotypic markers.

4.3. Clinical translation and potential applications

The translational implications of TKSI are broad. TKSI can inform patient selection in immunotherapy trials, especially those involving agents targeting STING, TLR9, or programmed cell death protein 1/PD-L1. It can also guide virome-specific adjuvant strategies, such as targeting HERV-K, modulating phage–TLR9 interactions, or interrupting the EBV miRNA–PD-L1 axis. Next-generation trial designs may include testing differential therapeutic benefit in TKSI-high and TKSI-low patients in Bayesian response-adaptive trials, modeled on BATTLE. Additionally, TKSI-informed mechanistic experiments could be used to test causality—for example, phage CpG-induced NF- κ B activation in TLR9+/+ vs. TLR9–/–; EBV miRNA–PD-L1 pathway validation via miRNA mimic transfection of EBV-negative organoids; and EMT induction by HERV-K assayed through short hairpin RNA-mediated env knockdown with readouts of MYC, vimentin, and E-cadherin. Although this research does not directly assert causality, it provides a rational framework for designing experimental research.

Finally, the possibility of extending the analysis to non-classical oncogenic viruses represents one key conceptual advance. Modeling phages and HERVs in addition to HPV and EBV expands the scope from a limited range of well-known oncogenic pathogens to the broader complexity of the human virome. Therapeutically, this creates actionable opportunities: TLR9 modulation to blunt phage-driven NF- κ B signaling; antagomirs to disrupt EBV-miRNA–PD-L1 coupling; HERV-K-specific chimeric antigen

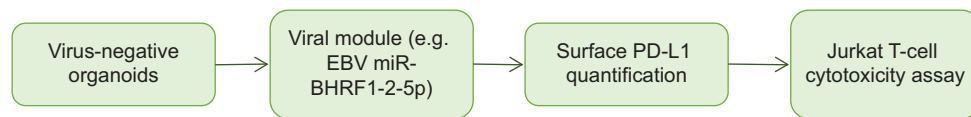


Figure 7. Experimental roadmap for validating host–virome couplings: A conceptual workflow outlining *in vitro*, *ex vivo*, and *in vivo* assays to test Trans-Kingdom Signaling Index-derived mechanistic predictions

Abbreviations: EBV: Epstein–Barr virus; PD-L1: Programmed death-ligand 1.

receptor T cells or monoclonal antibodies, which have shown promising preclinical efficacy in breast cancer;^{20,60,61} and context-dependent modulation of cGAS–STING to favor acute antitumor immunity while avoiding chronic immunosuppression. Collectively, these directions illustrate how direct manipulation of trans-kingdom signaling may reprogram tumor biology and open new avenues for therapy.

4.4. Experimental roadmap for validating trans-kingdom interactions

To enhance the translational utility of TKSI, we propose a future experimental roadmap to validate its predictions (Figure 7). This framework consists of:

- (i) Functional assays that evaluate individual viral modules, such as EBV miRNA mimic transfection, HERV-K knockdown, and phage CpG–TLR9 stimulation.
- (ii) Co-culture systems that measure immune-evasion phenotypes, such as PD-L1 upregulation and T-cell cytotoxicity.
- (iii) *In vivo* models that assess the causal effect of viral components on pathway activation and tumor progression.

This roadmap provides a stepwise methodology to empirically test the trans-kingdom signaling relationships described by TKSI.

4.5. Strengths of the TKSI framework

Key strengths of this study include (i) cross-cancer applicability, (ii) integration of multiviral and host pathway features, (iii) robust statistical validation using bootstrap CIs and cross-validation, and (iv) a coupling matrix explicitly grounded in mechanistic biology. The effective stratification of survival across three biologically distinct cancers demonstrates the versatility and potential clinical relevance of the framework.

5. Limitations

Several limitations remain in this study. First, the present study is based on bulk RNA-seq, which cannot resolve cell-type-specific viral activity or microenvironmental interactions. Second, although multiple tumor types were included, external cohorts with matched viral annotation were limited, thereby limiting definitive

external validation. Third, mechanistic couplings are well-grounded in existing literature and statistically sound, but without functional assays, causal inferences cannot be drawn. Fourth, virome detection depends on sequencing depth and the completeness of reference databases, potentially underestimating low-abundance viral signals. Lastly, although TKSI complements current immune scores, incorporation into larger multi-omics datasets (e.g., proteomics, single-cell analyses) would further enhance biological interpretation. These limitations do not diminish the analytic value of TKSI but highlight directions for future research.

6. Conclusion

This study developed and implemented a new mathematical model, TKSI, to assess the extent to which virome-derived signals modulate host cancer pathways. TKSI integrates the joint action of viral oncogenes, endogenous retroviruses, and bacteriophages into a single quantitative variable, providing an integrated, biologically informed framework to estimate trans-kingdom signaling dynamics in cancer. Patients with TKSI-high tumors consistently exhibited features of aggressive tumor biology, such as immune evasion, inflammatory activation, loss of tumor suppressor functions, immune-checkpoint interactions, and EMT, highlighting the index's ability to capture a reproducible molecular phenotype with clinical relevance.

The results reinforce prior observations that interactions between HPV E6/E7 and p53 are functionally stabilized, EBV enhances PD-L1, and other modulatory viral activities also influence tumor behavior. Collectively, these findings implicate the virome as an actively involved component in cancer development and establish TKSI as a strong prognostic tool with translational applications for patient stratification, biomarker identification, and prediction of immunotherapy response. Further empirical and prospective clinical data, along with additional functional validation, will be essential to determine the utility of TKSI in oncology as a virome-guided tool for informing prognosis and therapeutic decisions.

Acknowledgements

The authors sincerely thank the participating institutions and collaborators for their support throughout this study.

Special appreciation goes to Skyline University Nigeria for providing academic and technical guidance.

Funding

None.

Conflict of interest

The authors declare that they have no competing interests.

Author contributions

Conceptualization: Miracle Uwa Livinus, Mustapha Abdulsalam

Data curation: Musa Ojeba Innocent, Mustapha Abdulsalam, Madinat Hassan, Shehu Sani

Formal analysis: Musa Ojeba Innocent, Mustapha Abdulsalam, Madinat Hassan, Shehu Sani

Investigation: Mustapha Abdulsalam, Musa Ojeba Innocent, Stephen Olaide Aremu, Katimu Yusuf

Methodology: Miracle Uwa Livinus, Sunday Zeal Bala, Katimu Yusuf, Madinat Hassan

Writing – original draft: Miracle Uwa Livinus, Mustapha Abdulsalam, Sunday Zeal Bala, Stephen Olaide Aremu

Writing – review & editing: All authors

Ethics approval and consent to participate

This study was conducted in accordance with the Declaration of Helsinki. Ethical approval for the use of de-identified patient-derived datasets was originally obtained by contributing institutions, including The Cancer Genome Atlas and associated repositories. All data analyzed in this study were publicly available and fully anonymized; therefore, no additional patient consent was required.

Consent for publication

Not applicable.

Availability of data

Not applicable.

References

1. Liu B, Zhou H, Tan L, Siu KTH, Guan XY. Exploring treatment options in cancer: Tumor treatment strategies. *Signal Transduct Target Ther.* 2024;9(1):175.
doi: 10.1038/s41392-024-01856-7
2. Hassan M, Adegboyega TT, Bala SZ, *et al.* The carcinogenic risks of military explosives: Mechanisms, health impacts, and environmental consequences of chemical munitions. In: *Toxicology and Environmental Health Sciences*. Berlin: Springer Nature; 2025. p. 1-15.
doi: 10.1007/s13530-025-00256-w
3. Li X, Hua W, Xu W, Ning N. Oral microbiota: A new insight into cancer progression, diagnosis and treatment. *Phenomics.* 2023;3(5):535-547.
doi: 10.1007/s43657-023-00124-y
4. Faria M, Mónica T, Maria JP, Paulo S. Efficacy of acupuncture on cancer pain: A systematic review and meta-analysis. *J Integr Med.* 2024;22(3):235-244.
doi: 10.1016/j.joim.2024.03.002
5. Zhang S, Xiao X, Yi Y, *et al.* Tumor initiation and early tumorigenesis: Molecular mechanisms and interventional targets. *Signal Transduct Target Ther.* 2024;9(1):1-36.
doi: 10.1038/s41392-024-01848-7
6. Fernandes Q, Gupta I, Vranic S, Al Moustafa AE. Human papillomaviruses and Epstein-Barr virus interactions in colorectal cancer: A brief review. *Pathogens.* 2020;9(4):300.
doi: 10.3390/pathogens9040300
7. Liang G, Bushman FD. The human virome: Assembly, composition and host interactions. *Nat Rev Microbiol.* 2021;19(8):514-527.
doi: 10.1038/s41579-021-00536-5
8. Bautista J, Lopez-Cortes A. Oncogenic viruses rewire the epigenome in human cancer. *Front Cell Infect Microbiol.* 2025;15:1617198.
doi: 10.3389/fcimb.2025.1617198
9. Li Z, Gao J, Xiang X, Deng J, Gao D, Sheng X. Viral long non-coding RNA regulates virus life-cycle and pathogenicity. *Mol Biol Rep.* 2022;49(7):6693-6700.
doi: 10.1007/s11033-022-07268-6
10. Sarma A, Suri P, Justice M, Angamuthu R, Pushparaj S. Role of long non-coding RNAs in viral gene expression, pathogenesis, and innate immunity in viral chicken diseases. *Noncoding RNA.* 2025;11(3):42.
doi: 10.3390/ncrna11030042
11. Torres MKS, Pereira Neto GS, Cayres Vallinoto IMV, Reis LO, Vallinoto ACR. Impact of oncogenic viruses on cancer development: A narrative review. *Biology (Basel).* 2025;14(7):797.
doi: 10.3390/biology14070797
12. Samara P, Athanasopoulos M, Mastronikolis S, Kyrodimos E, Athanasopoulos I, Mastronikolis NS. Role of oncogenic viruses in head and neck cancers: Epidemiology, pathogenesis, and detection methods. *Microorganisms.* 2024;12(7):1482.
doi: 10.3390/microorganisms12071482
13. Feitelson MA, Arzumanyan A, Spector I, Medhat A. Hepatitis B X protein as a component of a functional cure for chronic hepatitis B. *Biomedicines.* 2022;10(9):2210.
doi: 10.3390/biomedicines10092210

14. da Silva AL, Guedes BLM, Santos SN, *et al.* Beyond pathogens: Genetic legacy of endogenous retroviruses in host physiology. *Front Cell Infect Microbiol.* 2024;14:1379962. doi: 10.3389/fcimb.2024.1379962
15. Russ E, Mikhalkovich N, Iordanskiy S. Expression of HERV-K HML-2 correlates with macrophage immune activation and type I interferon response. *Microbiol Spectr.* 2023;11(2):e0443822. doi: 10.1128/spectrum.04438-22
16. Logotheti S, Stiewe T, Georgakilas AG. Role of human endogenous retroviruses in cancer immunotherapy post-COVID-19. *Cancers (Basel).* 2023;15(22):5321. doi: 10.3390/cancers15225321
17. Cherkasova EA, Chen L, Childs RW. Regulation of HERV activation in tumors and implications for oncology. *Front Cell Infect Microbiol.* 2024;14:1358470. doi: 10.3389/fcimb.2024.1358470
18. Yao L, Rosanna RS, Elena RS, *et al.* Role of human endogenous retroviruses in melanoma initiation and progression. *Biomedicines.* 2025;13:1662. doi: 10.3390/biomedicines13071662
19. Alkhalil SS. Role of bacteriophages in shaping bacterial diversity in the human gut. *Front Microbiol.* 2023;14:1232413. doi: 10.3389/fmicb.2023.1232413
20. Chatterjee A, Duerkop BA. Beyond bacteria: bacteriophage-eukaryotic host interactions. *Front Microbiol.* 2018;9:1394. doi: 10.3389/fmicb.2018.01394
21. Islam MS, Fan J, Pan F. Power of phages in cancer treatment. *Front Oncol.* 2023;13:1290296. doi: 10.3389/fonc.2023.1290296
22. Zhao H, Wu L, Yan G, *et al.* Inflammation and tumor progression: Signaling pathways and interventions. *Signal Transduct Target Ther.* 2021;6(1):263. doi: 10.1038/s41392-021-00658-5
23. Mao H, Zhao X, Sun SC. NF- κ B in inflammation and cancer. *Cell Mol Immunol.* 2025;22(8):811-839. doi: 10.1038/s41423-025-01310-w
24. Wang Y, Zhu Y, Cao Y, *et al.* cGAS-STING activation in cancer therapy. *Front Immunol.* 2025;16:1579832. doi: 10.3389/fimmu.2025.1579832
25. Li Q, Wu P, Du Q, Hanif U, Hu H, Li K. cGAS-STING signaling in disease and therapy. *MedComm (2020).* 2024;5(4):e511. doi: 10.1002/mco2.511
26. Szpara ML, Van Doorslaer K. Mechanisms of DNA virus evolution. *Encycl Virol.* 2020;1-5:71-78. doi: 10.1016/B978-0-12-809633-8.20993-X
27. Gaudino M, Nagamine B, Ducatez MF, Meyer G. Understanding mechanisms of viral and bacterial coinfections in bovine respiratory disease: A comprehensive review. *Vet Res.* 2022;53(1):70. doi: 10.1186/s13567-022-01086-1
28. Rajagopala SV, Bakhoun NG, Pakala SB, *et al.* Metatranscriptomics to characterize respiratory virome, microbiome, and host response from clinical samples. *Cell Rep Methods.* 2021;1(6):100091. doi: 10.1016/j.crmeth.2021.100091
29. Siegel RL, Miller KD, Wagle NS, Jemal A. Cancer statistics, 2023. *CA Cancer J Clin.* 2023;73(1):17-48. doi: 10.3322/caac.21763
30. Duerkop BA, Hooper LV. Resident viruses and interactions with the immune system. *Nat Immunol.* 2013;14(7):654-659. doi: 10.1038/ni.2614
31. Notarte KI, Senanayake S, Macaranas I, *et al.* MicroRNA and other non-coding RNAs in Epstein-Barr virus-associated cancers. *Cancers (Basel).* 2021;13(15):3909. doi: 10.3390/cancers13153909
32. Moody CA, Laimins LA. Human papillomavirus oncoproteins: Pathways to transformation. *Nat Rev Cancer.* 2010;10(8):550-560. doi: 10.1038/nrc2886
33. Hayden MS, Ghosh S. Shared principles in NF- κ B signaling. *Cell.* 2008;132(3):344-362. doi: 10.1016/j.cell.2008.01.020
34. Motwani M, Pesiridis S, Fitzgerald KA. DNA sensing by the cGAS-STING pathway in health and disease. *Nat Rev Genet.* 2019;20(11):657-674. doi: 10.1038/s41576-019-0151-1
35. Wotherspoon D, Rogerson C, O'Shaughnessy RFL. Controlling epidermal terminal differentiation with transcriptional bursting and RNA bodies. *J Dev Biol.* 2020;8(4):29. doi: 10.3390/jdb8040029
36. Hänzelmann S, Castelo R, Guinney J. GSVA: Gene set variation analysis for microarray and RNA-seq data. *BMC Bioinformatics.* 2013;14:7. doi: 10.1186/1471-2105-14-7
37. Cristino AS, Nourse J, West RA, *et al.* EBV microRNA-BHRF1-2-5p targets immune checkpoint ligands PD-L1 and PD-L2. *Blood.* 2019;134(25):2261-2270. doi: 10.1182/blood.2019000889
38. Siying L, Hong X, Wei Z, *et al.* Ubiquitination of HPV oncoprotein E6 is critical for p53 degradation. *Front Microbiol.* 2019;10:2483.

- doi: 10.3389/fmicb.2019.02483
39. Zanier K, Mancas F, Paci A, *et al.* Structure of the E6/E6AP/p53 complex required for HPV-mediated p53 degradation. *Nature*. 2016;529(7587):541-545.
doi: 10.1038/nature16481
40. Lepej SZ, Matulić M, Gršković P, Pavlica M, Radmanić L, Korać P. miRNAs: EBV immune escape and tumorigenesis mechanisms. *Pathogens*. 2020;9(5):353.
doi: 10.3390/pathogens9050353
41. Li W, He C, Wu J, Yang D, Yi W. Epstein-Barr virus-encoded miRNAs assist host immune escape. *J Cancer*. 2020;11(8):2091-2100.
doi: 10.7150/jca.42498
42. Nakano H, Saito M, Nakajima S, *et al.* PD-L1 overexpression in EBV-positive gastric cancer via genomic and epigenomic mechanisms. *Sci Rep*. 2021;11(1):81667.
doi: 10.1038/s41598-021-81667-w
43. Lima A, Sousa H, Medeiros R, Nobre A, Machado M. PD-L1 expression in EBV-associated gastric cancer: Systematic review and meta-analysis. *Discov Oncol*. 2022;13(1):79.
doi: 10.1007/s12672-022-00479-0
44. Wonglhow J, Tantipisit J, Wetwittayakhleng P, *et al.* EBV infection and PD-L1 expression in gastric cancer. *Cancers (Basel)*. 2025;17(9):1492.
doi: 10.3390/cancers17091492
45. Miliotis CN, Slack FJ. Multi-layered control of PD-L1 expression in EBV-associated gastric cancer. *J Cancer Metastasis Treat*. 2020;6:12.
doi: 10.20517/2394-4722.2020.12
46. Ding L, Zhang R, Du W, Wang Q, Pei D. Role of the cGAS-STING signaling pathway in ferroptosis. *J Adv Res*. 2024;58:1-15.
doi: 10.1016/j.jare.2024.12.028
47. Wang Q, Yu Y, Zhuang J, Liu R, Sun C. Precision regulation of the cGAS-STING pathway in the tumor immune microenvironment. *Mol Cancer*. 2025;24(1):80.
doi: 10.1186/s12943-025-02380-0
48. Broecker F, Moelling K. Roles of the virome in cancer. *Microorganisms*. 2021;9(12):2538.
doi: 10.3390/microorganisms9122538
49. Santiago-Rodriguez TM, Hollister EB. Human virome and disease: Phage-bacteria dysbiosis in the human gut. *Viruses*. 2019;11(7):656.
doi: 10.3390/v11070656
50. Junli L, Fu L, Wang G, Subbian S, Qin C, Zhao A. Unmethylated CpG DNA from BCG promotes macrophage activation via TLR9. *Innate Immun*. 2020;26(3):183-203.
doi: 10.1177/1753425919879997
51. Li H, Liu S, Hu J, *et al.* Epstein-Barr virus lytic reactivation and carcinogenesis. *Int J Biol Sci*. 2016;12(11):1309-1318.
doi: 10.7150/ijbs.16564
52. Iempridee T, Das S, Xu I, Mertz JE. TGF- β -induced EBV reactivation via Smad-binding elements of BZLF1. *J Virol*. 2011;85(15):7838-7853.
doi: 10.1128/JVI.01197-10
53. Adamson AL, Darr D, Holley-Guthrie E, *et al.* EBV BZLF1 and BRLF1 activate ATF2 via p38 and JNK. *J Virol*. 2000;74(3):1224-1233.
doi: 10.1128/JVI.74.3.1224-1233.2000
54. Germini D, Sall FB, Shmakova A, *et al.* Oncogenic properties of the EBV ZEBRA protein. *Cancers (Basel)*. 2020;12(6):1479.
doi: 10.3390/cancers12061479
55. Yu X, Wang Z, Mertz JE. ZEB1 regulates the latent-lytic switch in Epstein-Barr virus infection. *PLoS Pathog*. 2007;3(12):e194.
doi: 10.1371/journal.ppat.0030194
56. Lopes de Sousa HM, Costa Ribeiro JP, Timóteo MB. *Epstein-Barr Virus-Associated Gastric Cancer: Old Entity with New Relevance*. London: IntechOpen; 2021.
doi: 10.5772/intechopen.93649
57. Mansouri S, Pan Q, Blencowe BJ, Claycomb JM, Frappier L. EBNA1 regulates EBV latency via let-7 microRNA and dicer. *J Virol*. 2014;88(19):11166-11177.
doi: 10.1128/JVI.01785-14
58. Damania B, Kenney SC, Raab-Traub N. Epstein-Barr virus: Biology and clinical disease. *Cell*. 2022;185(20):3652-3670.
doi: 10.1016/j.cell.2022.08.026
59. Salavatiha Z, Soleimani-Jelodar R, Jalilvand S. Role of endogenous retrovirus-K in human cancer. *Rev Med Virol*. 2020;30(6):e2142.
doi: 10.1002/rmv.2142
60. Lindsay AR, Himmel M, An MW, Daniel JS, Mandrekar SJ. Clinical trial designs incorporating predictive biomarkers. *Cancer Treat Rev*. 2016;43:74-82.
doi: 10.1016/j.ctrv.2015.12.008
61. Chew V, Chuang CH, Hsu C. Translational research on drug development and biomarker discovery for hepatocellular carcinoma. *J Biomed Sci*. 2024;31(1):22.
doi: 10.1186/s12929-024-01011-y